Identification of B Cells as a Major Site for Cyprinid Herpesvirus 3 Latency

Citation	Reed, A. N., Izume, S., Dolan, B. P., LaPatra, S., Kent, M., Dong, J., & Jin, L. (2014). Identification of B Cells as a Major Site for Cyprinid Herpesvirus 3 Latency. Journal of Virology, 88(16), 9297-9309. doi:10.1128/JVI.00990-14
DOI	10.1128/JVI.00990-14
Publisher	American Society for Microbiology
Version	Version of Record
Terms of Use	http://cdss.library.oregonstate.edu/sa-termsofuse

JVI Journals.ASM.org

Identification of B Cells as a Major Site for Cyprinid Herpesvirus 3 Latency

Aimee N. Reed,[a,b] Satoko Izume,[a] Brian P. Dolan,[a] Scott LaPatra,[c] Michael Kent,[a,b] Jing Dong,[a] Ling Jin[a,b]

Department of Biomedical Sciences, College of Veterinary Medicine, Oregon State University, Corvallis, Oregon, USA[a]; Department of Microbiology, College of Science, Oregon State University, Corvallis, Oregon, USA[b]; Research Division, Clear Springs Foods, Inc., Buhl, Idaho, USA[c]

ABSTRACT

Cyprinid herpesvirus 3 (CyHV-3), commonly known as koi herpesvirus (KHV), is a member of the *Alloherpesviridae*, and is a recently discovered emerging herpesvirus that is highly pathogenic for koi and common carp. Our previous study demonstrated that CyHV-3 becomes latent in peripheral white blood cells (WBC). In this study, CyHV-3 latency was further investigated in IgM$^+$ WBC. The presence of the CyHV-3 genome in IgM$^+$ WBC was about 20-fold greater than in IgM$^-$ WBC. To determine whether CyHV-3 expressed genes during latency, transcription from all eight open reading frames (ORFs) in the terminal repeat was investigated in IgM$^+$ WBC from koi with latent CyHV-3 infection. Only a spliced ORF6 transcript was found to be abundantly expressed in IgM$^+$ WBC from CyHV-3 latently infected koi. The spliced ORF6 transcript was also detected *in vitro* during productive infection as early as 1 day postinfection. The ORF6 transcript from *in vitro* infection begins at −127 bp upstream of the ATG codon and ends +188 bp downstream of the stop codon, +20 bp downstream of the polyadenylation signal. The hypothetical protein of ORF6 contains a consensus sequence with homology to a conserved domain of EBNA-3B and ICP4 from Epstein-Barr virus and herpes simplex virus 1, respectively, both members of the *Herpesviridae*. This is the first report of latent CyHV-3 in B cells and identification of gene transcription during latency for a member of the *Alloherpesviridae*.

IMPORTANCE

This is the first demonstration that a member of the *Alloherpesviridae*, cyprinid herpesvirus 3 (CyHV-3), establishes a latent infection in the B cells of its host, *Cyprinus carpio*. In addition, this is the first report of identification of gene transcription during latency for a member of *Herpesvirales* outside *Herpesviridae*. This is also the first report that the hypothetical protein of latent transcript of CyHV-3 contains a consensus sequence with homology to a conserved domain of EBNA-3B from Epstein-Barr virus and ICP4 from herpes simplex virus 1, which are genes important for latency. These strongly suggest that latency is evolutionally conserved across vertebrates.

Cyprinid herpesvirus 3 (CyHV-3), commonly known as koi herpesvirus (KHV), is a recently emerging pathogen of koi and common carp (*Cyprinus carpio*) that causes significant disease and high mortality in infected fish (1). The most prominent clinical signs from the active viral infection are seen in the gills, characterized by hyperplasia and severe necrosis of the gill epithelium. Other clinical signs include sunken eyes and pale patches on skin, ulcerative skin lesions, lethargy, anorexia, increased respiration, and uncoordinated swimming and movement; the disease is further characterized by interstitial nephritis, splenitis, and enteritis (2). Mortality rates have been reported as high as 80 to 100% in naive fry (3–5). Due to the severity of the disease, CyHV-3 has devastated the carp aquaculture population around the world and affected the koi trade, costing hundreds of millions of dollars in damage and loss.

CyHV-3 has been classified as a member of *Alloherpesviridae*, which consists of herpesviruses of fish and amphibians, and is in the order *Herpesvirales* (6, 7). Latency, a hallmark of herpesviruses, is the persistence of the viral genome in host cells for the life of the host in the absence of productive infection and viral replication. Reactivation from latency, largely triggered by physiologic host stressors, leads to virion production that produces clinical disease as well as transmission of the virus to naive hosts. CyHV-3 latency has also been demonstrated in koi that have recovered from an initial viral infection (8, 9).

Latency has classically been divided into establishment, maintenance, and reactivation phases. Although the mechanism of latency is not fully understood, it has been studied in many different herpesviruses: herpesviruses from animals, such as bovine herpesvirus type 1 (BHV-1), equine herpesvirus type 1, and porcine herpesvirus type 1 (10–13), and herpesviruses from humans, such as human herpesvirus type 1 and type 2 (herpes simplex virus 1 [HSV-1] and HSV-2), varicella-zoster virus (VZV), human cytomegalovirus (CMV), and Epstein-Barr virus (EBV) (13–15). In all the herpesviruses studied thus far, latency is characterized by a mostly dormant viral genome and limited gene expression. For alphaherpeviruses, such as HSV-1 and BHV-1, which become latent in the trigeminal ganglion, the only viral gene expressed during latency is the latency-associated transcript (LAT) or latency-related transcripts (LR) (11, 12, 16, 17). The LAT of *Simplexvirus*, such as HSV-1 (18) and HSV-2 (19), is expressed from the unique long inverted repeats, while the LR of the *Varicellovirus*, such as VZV (20), BHV-1 (11), and pseudorabies virus (PrV) (15), is ex-

Received 8 April 2014 **Accepted** 30 May 2014
Published ahead of print 4 June 2014
Editor: K. Frueh
Address correspondence to Ling Jin, ling.jin@oregonstate.edu.

doi:10.1128/JVI.00990-14

pressed from unique short inverted repeats. For betaherpesvirus latency, such as in human CMV (21, 22), a few more genes are reportedly expressed, such as the CMV latency transcripts, US28, viral interleukin 10 (vIL10), LUNA (latency unique natural antigen), and UL138 loci (23, 24). Although CMV has relatively short inverted repeats, the latency-associated UL138 loci (25) is close to the unique long inverted repeats. During gammaherpesvirus latency, in the case of EBV, up to nine virus-encoded proteins are expressed in latently infected B cells, which include the EBV nuclear antigens (EBNA-1, -2, -3A, -3B, -3C, and -LP) and the latent membrane proteins (LMP-1, -2A, and -2B) (26, 27). Most of the EBNAs are expressed from the repeat region near the end of the genome. In the case of Kaposi's sarcoma herpesvirus (KSHV), the major latency antigen (LANA [latency-associated nuclear antigen]) (28) is expressed from the direct repeat region 7 (DR7). Genes that are identified during latency can be divided into three groups: (i) transcription regulation, such as EBNA, which regulates viral gene expression during latency (27); (ii) antiapoptosis, such as LAT, which can block apoptosis during virus replication (29, 30); and (iii) immune modulation, such as vIL10, which can limit immune detection and mitigate clearance of latently infected cells (31, 32). These genes may have important roles in the establishment, maintenance, and reactivation of latency.

Although CyHV-3 is classified as a member of *Alloherpesviridae*, the biology of CyHV-3 latency and reactivation is unknown (9, 33). Understanding how CyHV-3 establishes latency in koi would provide information on the evolution of this seemingly conserved yet complex process. In this study, CyHV-3 latency was further investigated in IgM^+ white blood cells (WBC) and IgM^- WBC. To further prove that B cells are the preferred latency site, we investigated whether CyHV-3 transcribes any genes during latency. Since latency-associated genes from many herpesviruses are located in the inverted repeats, it is likely that CyHV-3 also expresses latency-associated genes from the inverted repeat region. Therefore, we chose to screen the inverted repeat region for genes associated with latency.

MATERIALS AND METHODS

Koi and sampling. Ten adult koi fish were acquired from a local distributor in Oregon with a history of CyHV-3 exposure. After a 30-day quarantine and acclimation period, fish found to have no clinical signs of CyHV-3 were used in our study. Koi with CyHV-3 latent infection were screened for CyHV-3 by nested PCR as reported previously (34). All koi were kept and maintained at 12°C in 4-ft diameter tanks at Oregon State University Salmon Disease Research Lab (OSU-SDL) in accordance with the Animal Care and Use Committee regulations. All blood samples were collected via venipuncture of the caudal vein after anesthetizing the koi with 90 ppm of MS-222 (tricaine methanesulfonate) buffered with an equal amount of sodium bicarbonate. Whole blood was immediately transferred into tubes containing 3.2% sodium citrate to prevent both coagulation and erythrocyte lysis.

CCB and KF-1 cell lines. Common carp brain cell line (CCB) and koi fin cell line (KF-1) (gift from Ronald Hedrick, University of California, Davis) were cultured in Dulbecco's modified Eagle's medium (DMEM) (Invitrogen, Carlsbad, CA) supplemented with 10% fetal bovine serum (Gemini Bio-Products, West Sacramento, CA), penicillin (100 U/ml), and streptomycin (100 μg/ml) (Sigma-Aldrich, Inc., St. Louis, MO) and incubated at 22°C. The United States strain of CyHV-3 (KHV-U) was a gift from Ronald Hedrick.

Antibodies. Anti-common carp IgM monoclonal antibody was purchased from Aquatic Diagnostics Ltd. (Stirling, Scotland, United Kingdom). Anti-mouse IgG microbeads were purchased from Miltenyi Biotec (Bergisch Gladbach, Germany). Anti-Pax5 polyclonal antibody specific to the paired domain of trout *Pax5* was a gift from Patty Zwollo (College of William and Mary) (35). The secondary antibodies used were as follows: DyLight 649-labeled donkey anti-mouse IgG antibody (Thermo Fisher Scientific, Rockford, IL), Alexa Fluor 488-labeled goat anti-rabbit IgG antibody (Molecular Probes, Eugene, OR), and Texas Red-labeled goat anti-mouse IgG antibody (Molecular Probes, Eugene, OR). Nuclear staining was performed with Vectashield mounting medium with 4′,6′-diamidino-2-phenylindole (DAPI) (Vector Laboratories, Burlingame, CA).

IgM^+ WBC isolation. White blood cells (WBC) were collected after layering whole blood on a Ficoll-Paque Plus gradient according to the manufacturer's instructions (GE Healthcare, United Kingdom) and washed twice with Hanks balanced salt solution (HBSS). Total WBC were stained first with anti-carp IgM monoclonal antibody (Aquatic Diagnostics Ltd.) at 1:100 dilution on ice for 60 min and rinsed twice with HBSS. WBC were then stained with anti-mouse IgG microbeads (Miltenyi Biotec) at a 1:4 dilution at 4°C for 30 min and washed once. Stained WBC were passed through an LS column on a magnet according to the manufacturer's instructions (Miltenyi Biotec, Bergisch Gladbach, Germany). The nonselected cells that flowed through the magnetized column were collected and labeled "IgM^- WBC"; the column was then removed from the magnet, and selected cells were washed off the column, collected, and labeled "IgM^+ WBC."

Flow cytometry and confocal microscopy. Populations of presorted WBC, IgM^+ WBC, and IgM^- WBC were analyzed by fluorescence-activated cell sorting (FACS) and confocal microscopy. Each population of cells was fixed with 4% paraformaldehyde and permeabilized with 0.1% saponin buffer in phosphate-buffered saline (PBS) with 1% bovine serum albumin (BSA). Each population was then stained with primary anti-carp IgM monoclonal antibody and anti-Pax5 polyclonal antibody (from rabbit) at 1:100 dilutions at 4°C for 30 min and rinsed twice with saponin buffer. The cells were then stained with secondary DyLight 649-labeled donkey anti-mouse IgG antibody and Alexa Fluor 488-labeled goat anti-rabbit IgG antibody at 1:500 dilution. A subset of each cell population was stained with only secondary antibodies to serve as a negative control. Stained cells were then analyzed by FACS with the BD Accuri C6 flow cytometer, and 20,000 events were recorded for each cell population. Data were analyzed with BD Sampler Analysis software. For visualization by confocal microscopy, cells were stained with secondary Texas Red-labeled goat anti-mouse IgG antibody and Alexa Fluor 488-labeled goat anti-rabbit IgG antibody at 1:500 dilution. DAPI was applied to cells before imaging for nucleus visualization. The cells were then examined with a Zeiss LSM510 Meta Axiovert 200 motorized microscope with LSM software v3.2. Confocal images were analyzed with ImageJ software v1.46r.

Total DNA and RNA extraction from WBC or CCB cells. Total DNA was extracted from an equal number of cells from IgM^+ and IgM^- WBC using the High Pure PCR template preparation kit (Roche Diagnostics, Indianapolis, IN) according to the manufacturer's instructions. Total RNA was extracted from IgM^+ and IgM^- WBC populations using TRIzol (Life Technologies, Carlsbad, CA) according to the manufacturer's instructions. Total RNA from *in vitro* infection was extracted from CCB cells infected with CyHV-3 at a multiplicity of infection (MOI) of 1 and harvested at 1, 3, 5, 8, 13, and 21 days postinfection with TRIzol.

Primers. Selection of primers for CyHV-3 sequence amplification was based on DNA sequences of CyHV-3 (NCBI accession no. NC_009127.1) available at NCBI. The primers used for screening for the presence of CyHV-3 DNA in koi WBC were selected as previously described (34). Real-time PCR primers specific for CyHV-3 were selected as previously described (2). The primers and TaqMan probe for *Cyprinus carpio* glucokinase gene were selected as reported previously (2). The primers used for screening open reading frame 1 (ORF1) to ORF8 gene expression during latency are shown in Fig. 1 and Table 1. The 3′ rapid amplification of cDNA ends (3′ RACE) primer and 5′ RACE primers are also shown in Fig. 1 and Table 1.

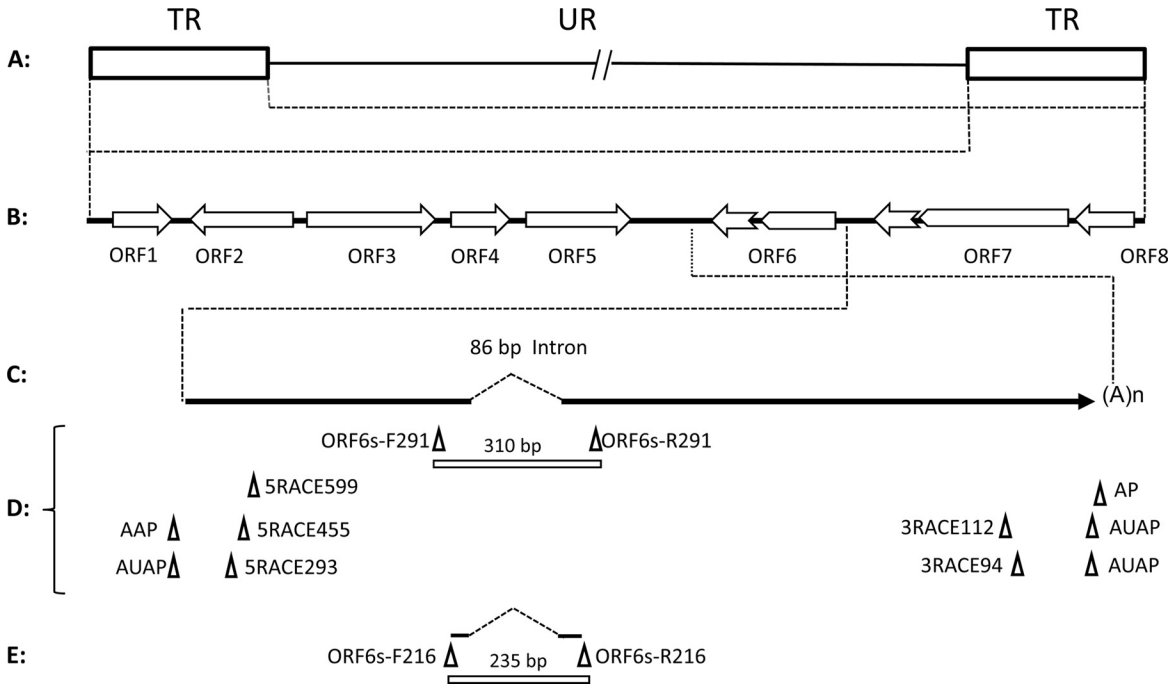

FIG 1 Schematic of CyHV-3 genome and locations of primers and DNA probe. (A) CyHV-3 genomic structure. The viral terminal repeats (TR) (containing ORF1 to ORF8) and unique regions (UR) containing ORF9 to ORF156 are indicated. (B) Expanded TR with ORF1 to -8; notched arrows indicate introns for ORF6 and ORF7. (C) Expanded 5′-3′ ORF6. The dashed line indicates the 86-bp intron. (D) Relative locations of the primers used in 5′ RACE and 3′ RACE and primers specific for the ORF6 flanking the intron. (E) Relative locations of the DNA probe specific for the spliced and unspliced ORF6. The expected sizes of the PCR products for the spliced ORF6 are indicated above the bars for primers ORF6s-F291 and -R291 or primers ORF6s-F216 and -R216.

TABLE 1 Primer pairs used in RT-PCR, PCR, and RACE

Assay	Primer[a]	KHV target	Primer sequence (5′ to 3′)
RT-PCR	ORF1-F340	ORF1	TGAGCACAGGACTGCTGATT
	ORF1-R430		AGGGACCAGGGTCTTCATCT
	ORF2-F377	ORF2	ATCATGGTCTGGCTGAGGAC
	ORF2-R377		GAGATATCCCCTGCCACTGA
	ORF3-F433	ORF3	AGCTGCTGAGAAAGCTGAGG
	ORF3-R433		CCAGGTGCAGAGTTGTCAGA
	ORF4-F399	ORF4	TGGTTCCTATGGCTGGGTAG
	ORF4-R399		CCGTCTCTGGGATGAGTGTT
	ORF5-F365	ORF5	TCAGCAGGACCAGGACTCTT
	ORF5-R365		ACAGCTCGTCGTACACGTTG
	ORF6s-F291	ORF6	GACCCAGGGGACAGCTCTAT
	ORF6s-R291		AGTGGTACAAGTGGCGCTTC
	ORF7s-F316	ORF7	CATCACTCAGCTGTGCCACT
	ORF7s-R316		CGCAAGAGAGCAGTGATGAA
	ORF8-F360	ORF8	TAAGACGTCGTGCTGTCAGG
	ORF8-R360		CAGGCTGAAGTGTGAGGTGA
Southern blotting	ORF6s-F216	ORF6	CAGCAGACTGAGACGCTGAA
	ORF6s-R216		TGCACCATGGACAGACAGAT
RACE	ORF6-3RACE112	ORF6	AAGAAGCACAGGAGCGAGAG
	ORF6-3RACE94		AGGGAGAGGAGCGAGAAGAG
	ORF6-5RACE599		GTGAACTGCACCCAGTCAAA
	ORF6-5RACE455		GTGCCCAGCTCAAACTTCTC
	ORF6-5RACE293		GCAACAGCGTGTCTCTGGTA

[a] The letter after the hyphen indicates whether a primer is forward (F) or reverse (R).

DNA probe. ORF6 reverse transcriptase PCR (RT-PCR) products amplified with primers ORF6s-F291 (s stands for spliced, and F stands for forward) and ORF6s-R291 (R stands for reverse) were cloned into the TOPO TA vector (Life Technologies, Carlsbad, CA). The plasmid containing the spliced ORF6 DNA at 310 bp (versus 396 bp of unspliced DNA) was confirmed by DNA sequencing. The ORF6 plasmid DNA was used as the template to generate the digoxigenin (DIG)-labeled DNA probe as shown in Fig. 1E. The DIG-labeled probe was made by PCR with primers ORF6s-216F and ORF6s-216R using the DIG DNA labeling kit according to the manufacturer's instructions (Roche Diagnostics, Indianapolis, IN).

PCR amplification. PCR was performed in a 25-μl reaction mixture consisting of 0.5 unit of AmpliTaq Gold 360 and 12.5 μl of 2× buffer (Life Technologies, Carlsbad, CA), 5 μl Q-solution enhancer (Qiagen, Germantown, MD), 400 μM each primer, and 0.5 μg of DNA or 2 μl of RT product. The mixture was subjected to the following steps: (i) 94°C for 2 min; (ii) 35 cycles, with 1 cycle consisting of 94°C for 30 s, 58°C for 30 s, and 72°C for 45 s; (iii) a 5-min elongation step at 72°C after the final cycle. The nested PCR was ran by using the same conditions as described above, the nested set of primers, and 2 μl of the PCR product as the template. Products were visualized on a 1.2% agarose gel with electrophoresis at 80 V and stained with ethidium bromide.

Real-time qPCR. CyHV-3 DNA was quantified in each sample by real-time PCR using primers KHV 86F and KHV 163R and TaqMan probe KHV 109P (2). Amplification was performed on the Bio-Rad CFX96 thermocycler (Bio-Rad Laboratories, Hercules, CA) using a 25-μl reaction mixture consisting of 12.5 μl Platinum quantitative PCR (qPCR) Supermix-UDG with ROX (Invitrogen, Carlsbad, CA), 0.5 μl of each primer (20 nM) and probe (10 mM), and 5 μl (approximately 1 μg total) of DNA template; the reaction mixture was subjected to the following steps: (i) 50°C for 2 min; (ii) 95°C for 2 min; (iii) 60 cycles, with 1 cycle consisting of 95°C for 15 s and 60°C for 60 s (a slower ramp time was

adjusted to 2°C/s to facilitate higher sensitivity). Data analysis was performed using the associated CFX Management Software suite (Bio-Rad Laboratories, Hercules, CA).

RT-PCR. Extracted RNA was treated with DNase (Life Technologies, Carlsbad, CA) according to the manufacturer's instructions before use in RT-PCR. cDNA was synthesized with either random primers or gene-specific primers using SuperScript III cDNA synthesis kit (Life Technologies, Carlsbad, CA) according to the manufacturer's instructions. As an internal control, an equal amount of RNA was treated in parallel without the addition of reverse transcriptase. The cDNA was subsequently amplified in PCR using primers specific for ORF1 to ORF8 listed in Table 1. RT-PCR products were visualized on a 1.2% agarose gel with electrophoresis at 80 V and stained with ethidium bromide. The 18S rRNA amplification was performed as an internal control to ensure that comparable levels of input RNA were used in RT-PCR, according to the manufacturer's instructions (QuantumRNA classic II universal 18S internal standard kit; Ambion, Life Technologies, Carlsbad, CA).

Southern blotting. RT-PCR products generated from RNA from IgM^+ or IgM^- WBC were electrophoresed through a 1.5% agarose gel, transferred to a nylon membrane (17), and then UV cross-linked to the membrane. The membrane was prehybridized with prehybridization buffer (Roche Diagnostics, Indianapolis, IN) at 68°C, and then hybridized with the DIG-labeled DNA probe specific for ORF6 (Fig. 1E) at 68°C overnight. After incubation with the probe, the membranes were washed with 0.1% sodium dodecyl sulfate and 10% 20× SSC (1× SSC is 0.15 M NaCl plus 0.015 M sodium citrate) before incubation with an anti-digoxigenin antibody conjugated with peroxidase. The membrane was then developed by incubation with a chemiluminescent peroxidase substrate (Roche Diagnostics, Indianapolis, IN). The blots were exposed to film (Kodak) at room temperature for 30 min to 2 h. The molecular sizes of the resulting bands were estimated by DNA Molecular Weight Marker VII (DIG labeled) (Roche Applied Science, Indianapolis, IN).

3′ RACE. The 3′ end of the ORF6 transcript was analyzed by the 3′ RACE system (Life Technologies, Carlsbad, CA) according to the manufacturer's instructions. Briefly, cDNA synthesis was performed in a 20-μl reaction mixture consisting of 1 μg of DNase-treated RNA isolated from CyHV-3-infected CCB cells was combined with the following: 2 μl of 10× PCR buffer; 500 nM adapter primer (AP); 500 μM each dATP, dCTP, dGTP, and dTTP; 10 mM dithiothreitol (DTT); and 2.5 mM $MgCl_2$. The reaction mixture was incubated at 42°C for 5 min before 1 μl of SuperScript RT II was added. The reaction mixture was then incubated at 42°C for 50 min. The reaction was terminated by heating the mixture at 70°C for 15 min. The resulting poly(dT) cDNA was treated with RNase H and incubated at 37°C for 20 min. Two microliters of this cDNA was used to amplify 3′ RACE products by PCR as described above, using 200 nM abridged universal amplification primer (AUAP) and 400 μM gene-specific primer ORF6-3RACE112 in the first reaction, and 2 μl of the PCR product was amplified again with the AUAP and seminested gene-specific primer ORF6-3RACE94.

5′ RACE. The 5′ end of the ORF6 transcript was mapped by the 5′ RACE system (Life Technologies). First-strand cDNA synthesis was conducted as described above with the gene-specific primer ORF6-5RACE599, and cDNA was treated with RNase H as described above. cDNA was purified by the protocol modified for the Roche high pure PCR product purification kit (Roche, Indianapolis, IN); the purified cDNA was then tailed with dCTP by terminal deoxynucleotidyl transferase (TdT) according to the manufacturer's instructions. The 5′ end of the ORF6 transcript was amplified first with primers ORF6-5RACE455 and AAP (abridged anchor primer) and then with AUAP and seminested primer ORF6-5RACE293 (Fig. 1D) as described above for 3′ RACE products.

PCR DNA sequencing. PCR products were cleaned with the ChargeSwitch PCR clean-up kit (Life Technologies, Carlsbad, CA) according to the manufacturer's instructions and submitted for Sanger sequencing at the Center for Genome Research and Bioinformatics (CGRB) at Oregon State University, Corvallis, OR. RT-PCR products were cloned using the TOPO TA vector (Invitrogen, Carlsbad, CA), and plasmids were submitted for Sanger sequencing at the CGRB. Sequences were aligned to the CyHV-3 genome by using Geneious software.

RESULTS

Isolation of koi B cells. In a previous study, we tentatively identified the peripheral WBC as the latency site for CyHV-3 (9). To determine which leukocyte population harbors latent CyHV-3, the peripheral WBC of koi were further sorted into IgM^+ and IgM^- WBC using magnetic beads to isolate cells labeled with an anti-carp IgM monoclonal antibody. Pooled WBC isolated from whole blood collected from five koi (2 ml from each fish) were stained first with the antibody and separated via a magnetic column (Miltenyi Biotec). On average, about 25% of total WBC were selected by the magnetic beads. To confirm that selection was specific for IgM^+ B cells, presorted WBC, IgM selected, and nonselected cells were costained by antibodies against IgM and transcription factor Pax5, an additional marker specific for B cells (36), and analyzed by FACS. As shown in Fig. 2A, before the cells were sorted, the IgM^+ portion of the total WBC population was about 26.8%, the $Pax5^+$ cells were 25.0%, and the portion positive for both IgM and Pax5 was about 19.1% of total WBC (Fig. 2A). The results of the FACS analysis confirm that the magnetic column is capable of isolating the majority of IgM^+ WBC. Of the cells that were selected via a magnetic column, the portion that was IgM^+ was 96.5%, the portion that was $Pax5^+$ was 94.1%, and the portion that was positive for both IgM and Pax5 was 92.9% (Fig. 2B). Of the nonselected cells, only 14.0% were IgM^+, while 16.4% of cells were $Pax5^+$ (Fig. 2C). The vast majority of magnetically selected cells were identified as doubly positive for IgM and Pax5 by FACS, which confirms them as an enriched population of B lymphocytes. The coexpression of these two B cell markers in these WBC was also examined by confocal microscopy. In agreement with the FACS analysis, the majority of magnetically selected WBC had IgM staining on the cell surface and Pax5 staining localizing to the nucleus (Fig. 3A). In the IgM^+ portion of WBC, a small portion of cells had IgM^+ staining without Pax5 staining. Very few nonselected cells had IgM surface staining and Pax5 staining (Fig. 3B), and only a small portion of unsorted cells had IgM and Pax5 staining (Fig. 3C).

CyHV-3 genome assessment in IgM^+ B cells and IgM^- WBC. To determine what type of leukocyte is preferentially targeted in CyHV-3 latent infection, real-time PCR was used to compare CyHV-3 genome copy numbers between IgM^+ B cells and IgM^- WBC isolated from latently infected koi. Genome copy numbers from real-time PCR were extrapolated from a standard curve established by using 10-fold serial dilutions of CyHV-3 DNA from 10^9 to 10^5 genome copies (Fig. 4A). Real-time PCR was performed with an equal amount of DNA from IgM^+ B cells and IgM^- WBC and demonstrated that the presence of CyHV-3 genomes in IgM^+ B cells was about 20-fold more abundant than in IgM^- WBC (Fig. 4B, white bars). Comparable levels of *Cyprinus carpio* glucokinase gene were amplified from both IgM^+ and IgM^- populations of WBC when evaluated by real-time PCR, confirming equal amounts of DNA were examined in each sample (Fig. 4B, hatched bars).

Viral gene expression in latently infected B cells. To investigate whether CyHV-3 has any gene expression during latency, all eight open reading frames (ORFs) from the terminal repeat were investigated by RT-PCR (Fig. 1 and Table 1). Total RNA was ex-

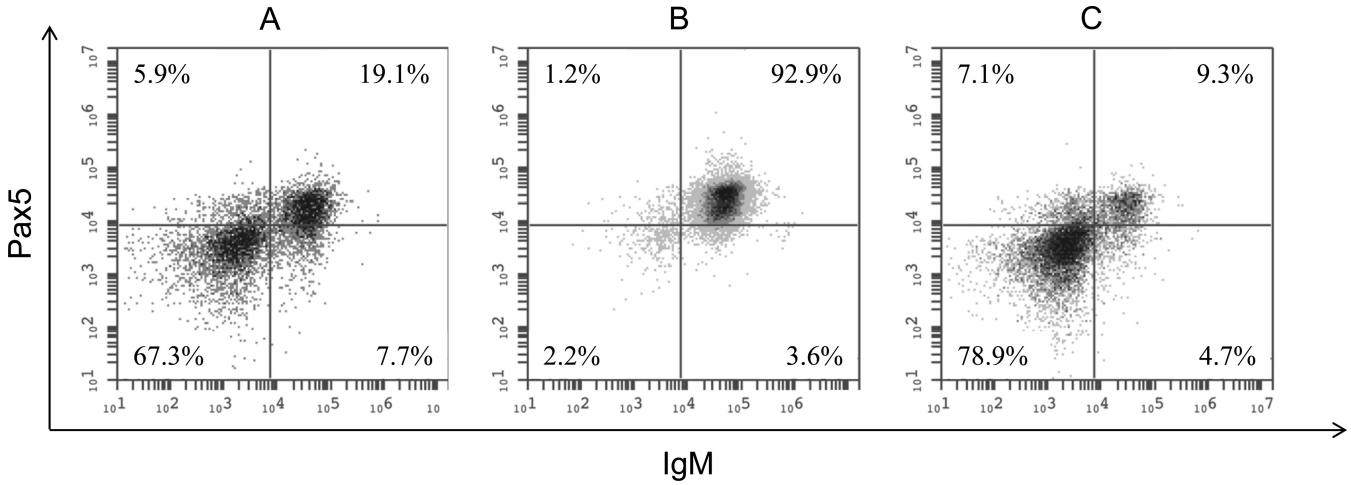

FIG 2 Fluorescence-activated cell staining (FACS) of koi peripheral WBC. After the cells were sorted on a magnetic column, they were stained with a mouse anti-carp IgM antibody and polyclonal rabbit anti-Pax5 antibody, followed by a secondary goat anti-rabbit IgG antibody which fluoresces at 488 nm (fluorescence intensity measured on the *y* axis) and secondary donkey anti-mouse IgG antibody which fluoresces at 649 nm (fluorescence intensity measured on the *x* axis). A total of 20,000 events were recorded for each cell population. (A) Peripheral WBC before magnetic sorting; (B) IgM$^+$ cells selected by the magnetic column; (C) IgM$^-$ nonselected cells that passed through the magnetic column.

tracted from IgM$^+$ B cells from latently infected koi and used in cDNA synthesis with random primers, which were then used in RT-PCR with primers specific for ORF1 to ORF8 (Fig. 1B and Table 1). Amplification from ORF1 to -5 and ORF7 to -8 was not observed (data not shown). However, using primers ORF6s-F291 and ORF6s-R291 flanking the intron of ORF6 (Fig. 1D), a spliced transcript was detected in IgM$^+$ B cells from latently infected koi. To confirm that the amplimer is the spliced ORF6 transcript, the RT-PCR product was hybridized with a DNA probe specific for the spliced ORF6 by Southern blotting (Fig. 1E and 5). In the RT reaction with reverse transcriptase, a spliced product of 310 bp was hybridized by the ORF6 probe (Fig. 5, lane 1). In the RT reaction without reverse transcriptase, an unspliced product of 396 bp was also hybridized by the probe, which may be derived from the genomic CyHV-3 DNA amplification (Fig. 5, lanes 2 and 4). No spliced DNA product was hybridized by the ORF6 probe in the RT-PCR from IgM$^-$ cells (Fig. 5, lane 3). Both spliced and unspliced ORF6 transcripts were amplified from total RNA from CyHV-3-infected CCB cells (Fig. 5, lane 7); however, only unspliced product was amplified from RNA from CyHV-3-infected CCB cells without the addition of reverse transcriptase, which may also come from the genomic DNA or the unspliced transcript (Fig. 5, lane 6). Since the spliced product is only about 86 bp shorter than the unspliced product, they are too close to clearly be sepa-

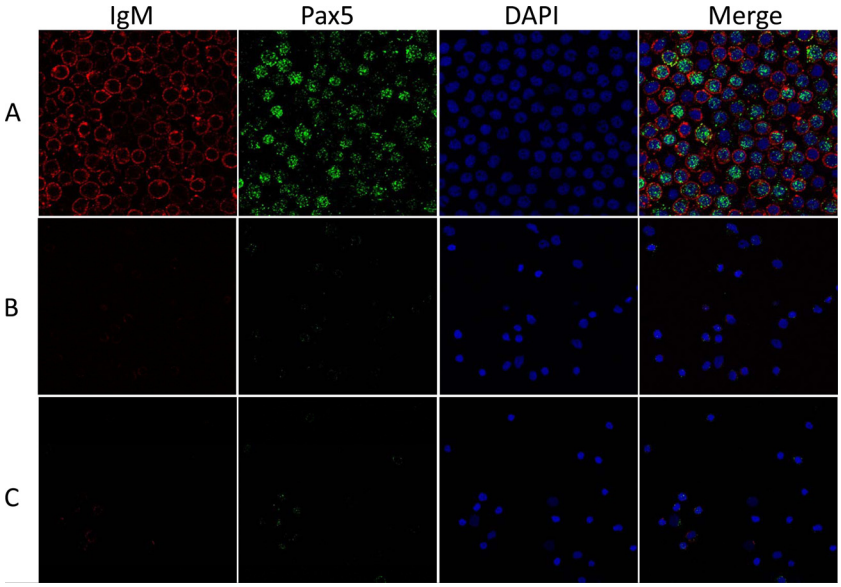

FIG 3 Confocal micrographs of koi peripheral WBC. IgM$^+$ cells were identified by anti-carp IgM monoclonal antibody and secondary goat anti-mouse IgG coupled with Texas Red (red). Pax5$^+$ cells were identified by anti-Pax5 polyclonal antibody and secondary goat anti-rabbit IgG antibody coupled with Alexa Fluor 488 (green). The nucleus was identified with DAPI (blue). The Merge images shows cells visualized by all three staining methods. (A) IgM$^+$ WBC selected by magnetic column; (B) IgM$^-$ nonselected cells that passed through magnetic column; (C) peripheral WBC before the cells were sorted on the magnetic column.

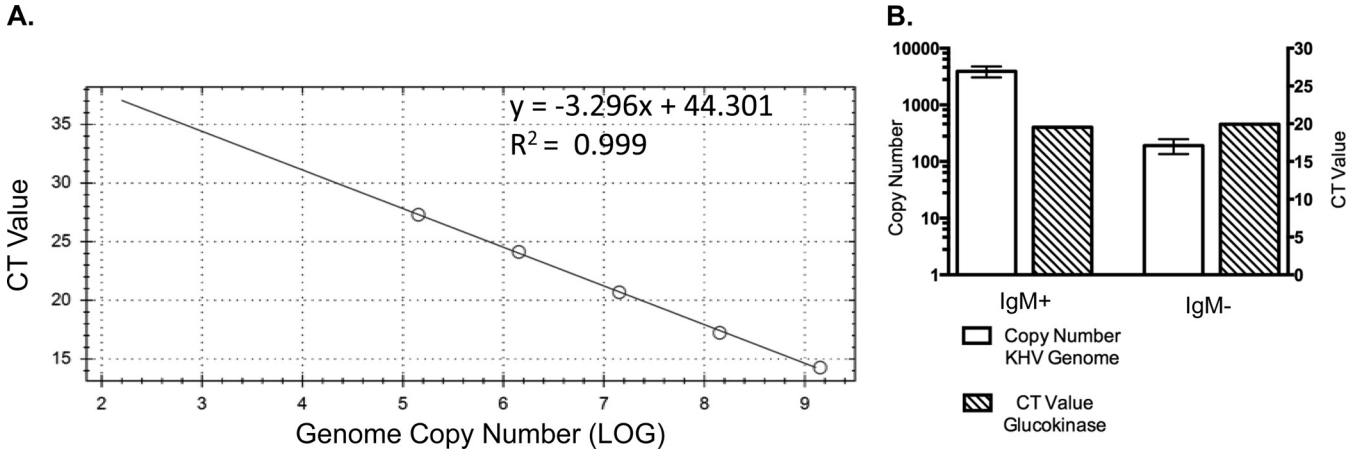

FIG 4 Real-time PCR of koi WBC DNA. (A) Standard curve using threshold cycles to calculate the analytic sensitivity of CyHV-3 genome equivalents with the real-time TaqMan PCR. (B) The white bars show the copy number of CyHV-3 genomes detected from 1×10^6 cells of selected (IgM^+ B cells) and nonselected (IgM^-) WBC from CyHV-3 latently infected koi. The mean genome copy numbers were 3,917.0 ± 496.0 for IgM^+ cells and 191.9 ± 32.4 for IgM^- cells ($n = 3$) ($P = 0.0017$ by two-tailed t test). The cycle threshold (C_T) values for the *Cyprinus carpio* glucokinase housekeeping gene from 1×10^6 cells from selected (IgM^+ B cells) and nonselected (IgM^-) WBC from CyHV-3 latently infected koi. The mean C_T values of the *Cyprinus carpio* glucokinase housekeeping gene were 19.55 ± 0.055 for IgM^+ cells and 19.93 ± 2.78 for IgM^- cells ($n = 2$) ($P = 0.9026$ by two-tailed t test).

rated on the gel (Fig. 5, lane 7). The unspliced DNA amplification control is KHV-U DNA (Fig. 5, lane 5). No product was amplified from the control reaction mixture containing no RNA template (Fig. 5, lane 8).

Expression of ORF6 transcript during productive infection of cultured cells. To determine whether ORF6 is expressed during productive infection, ORF6 transcription was investigated in CyHV-3 infection *in vitro*. Total RNA was extracted from CyHV-3-infected CCB cells or mock-infected CCB cells on days 1, 3, 5, 8, 13, and 21 postinfection (p.i.) and reverse transcribed to cDNA using the gene-specific primer ORF6s-R291. Spliced and unspliced ORF6 cDNA was detected via PCR with primers ORF6s-F291 and ORF6s-R291 designed to amplify a 310-bp spliced sequence or a 396-bp unspliced sequence spanning the intron region of the ORF6 (Fig. 1D). To confirm specificity of the ORF6 detection, the RT-PCR product was probed by a DIG-labeled DNA probe specific for ORF6 (Fig. 1E). A 310-bp product, the spliced ORF6, could be detected at 1 day p.i. (Fig. 6A and B, 1 dpi). Thereafter, the spliced transcript was detected in CyHV-3-infected CCB cells until 21 days p.i. (Fig. 6A and B). A 396-bp product, the unspliced ORF6, could be detected at 5 days p.i. and thereafter until 21 days p.i. Both spliced and unspliced transcription increased over the progression of viral infection, with strongest expression at days 13 p.i. (Fig. 6A). Comparable 18S RNA amplifications were observed in RNA samples from either CyHV-3-infected cells or mock-infected cells examined from different time points (Fig. 6C and F). Amplification did not occur when reverse transcriptase was omitted from the RT reaction (Fig. 6A) or when amplification was performed on RNA from mock-infected cells (Fig. 6D). No products were hybridized when reverse transcriptase was omitted from the RT reaction (Fig. 6B) or from amplification of RNA from mock-infected cells (Fig. 6E). Thus, the spliced ORF6 transcript is expressed immediately following infection.

Sequence analysis of the ORF6 RT-PCR products. To determine whether the intron boundary is as predicted by the sequence annotation, the spliced RT-PCR products from CyHV-3-infected CCB cells were sequenced directly by Sanger sequencing. The RT-PCR product from latently infected IgM^+ B cells (Fig. 6) was cloned into the TOPO-TA vector and then sequenced by Sanger

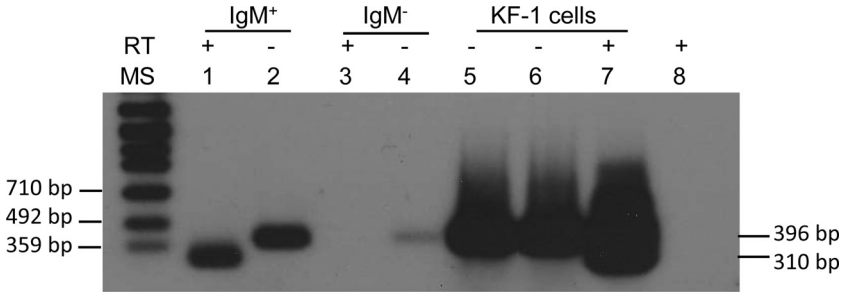

FIG 5 Autoradiogram of CyHV-3 ORF6 RT-PCR amplicons. cDNA was synthesized with random primer from total RNA of leukocytes isolated from CyHV-3 latently infected koi: sorted IgM^+ WBC (B cells) (lanes 1 and 2), IgM^- WBC (lanes 3 and 4) and KF-1 infected cells (lanes 6 and 7). Lane 5 is the positive control and contains CyHV-3 KHV-U DNA. Lane 8 is the negative control without nucleic acid). The presence (+) or absence (−) of reverse transcriptase (RT) in the cDNA synthesis reaction is shown. The PCR primers are ORF6s-F291 and ORF6s-R291. The membrane was probed with DIG-labeled DNA probe described in the legend to Fig. 1E, which is specific for ORF6 and internal to RT-PCR primers. The leftmost lane (lane MS) contains DNA Molecular Weight Marker VII (DIG labeled) (Roche Applied Science). The positions of the molecular size markers (in base pairs) estimated by using the molecular weight markers are indicated at the sides of the gel.

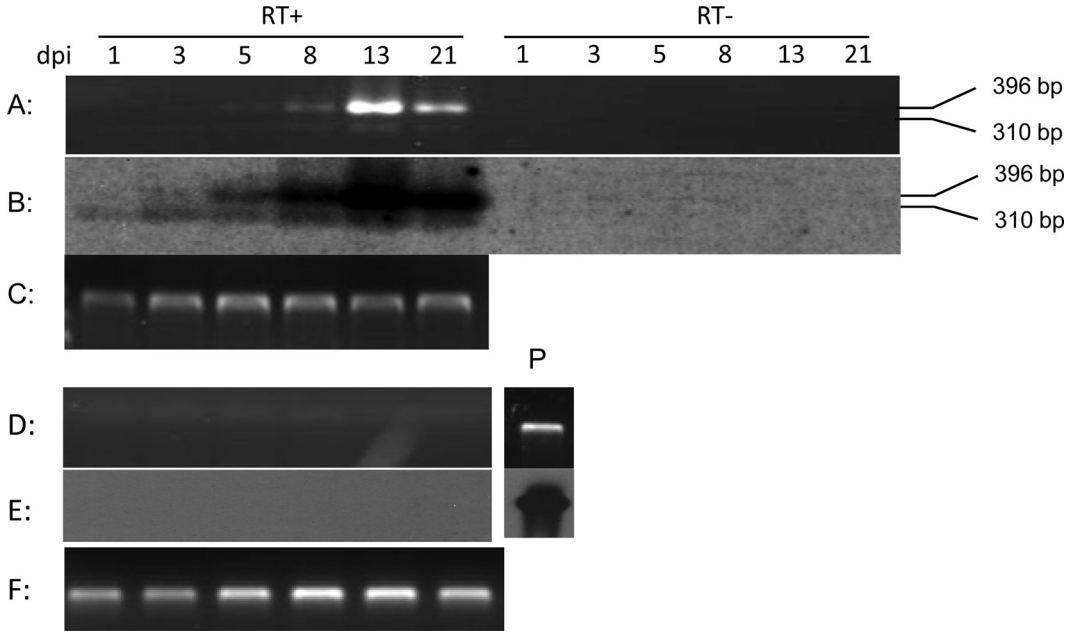

FIG 6 Temporal expression of ORF6 during CyHV-3 infection in CCB cells. (A and D) RT-PCR using total RNA harvested from infected CCB cells (A) or mock-infected cells (D) at 1, 3, 5, 8, 13, and 21 days postinfection (dpi) in the presence (RT+) or absence (RT−) of reverse transcriptase. The cDNA was synthesized with ORF6-specific primer ORF6s-R291. (B and E) Southern blot of RT-PCR in panel A (B) and panel D (E), probed with DIG-labeled ORF6 DNA probe described in the legend to Fig. 1E. The positions of the spliced product (310 bp) and unspliced product (396 bp) are indicated. (C and F) RT-PCR amplification of 18S rRNA showing 324-bp product from each time point as in panels A and D. The CyHV-3 DNA positive control (P) is shown.

sequencing. As shown in Fig. 7, the 86-bp intron boundary from both active and latent infection was identical to the predicted boundary (37). The amplimers generated from the total RNA of infected CCB and latent IgM$^+$ B cells were found to have over 99% homology with the corresponding region of the processed ORF6 (Fig. 7).

ORF6 predicted amino acid conserved domains. To investigate the putative function of this predicted 725-amino-acid (aa) ORF6, a search of conserved protein domains was performed (38). The amino acid sequence was submitted to the Conserved Domain Database (www.ncbi.nlm.nih.gov/Structure/cdd/cdd.shtml) and queried against the database PRK v6.9, which encompasses 10,885 PSSMs (position-specific scoring matrixes) and compounds conserved domain footprints from phage (PHA) proteins. As shown in Fig. 8, predicted ORF6 residues 347 to 472 have homology to the EBNA-3B consensus domain (Epstein-Barr virus nuclear antigen 3B; PHA03378; multidomain hit; bit score of 41.59; E value of 8.73e−04; pssmid 223065) between residues 683 and 808. This consensus domain is derived from three gammaherpesvirus proteins (39–41). The same region of the predicted ORF6 aa sequence (residues 342 to 468) also showed homology to multidomains of the herpesvirus transcriptional regulator protein ICP4 consensus domain (PHA03307; multidomain hit; bit score of 38.23; E value of 9.14e−03; pssmid 223039) between residues 103 and 225. This consensus domain is derived from 36 alphaherpesvirus proteins (42).

Characterizing the viral ORF6 transcript. To define the 5′ end of ORF6 RNA expressed *in vitro*, 5′ RACE was used. Total RNA isolated from CyHV-3-infected CCB cells at 13 days p.i. was analyzed. Primer 5RACE599, complementary to the DNA sequence 599 bp downstream of the ATG codon of ORF6, was used for the first-strand cDNA synthesis (Fig. 1D). Primers 5RACE455 and 5RACE293 upstream of primer 5RACE599 were used in PCR with AAP and AUAP (abridged universal amplification primer), respectively (Fig. 1D). No visible PCR product was observed when the primer pair AAP and 5RACE455 was used (Fig. 9A, lane 1). However, an approximately 400-bp product could be readily observed when the primary PCR product was reamplified with AUAP and the seminested primer 5RACE293 (Fig. 9A, lane 2). Sequencing of the 417-bp product revealed that the ORF6 transcript starts −127 bp upstream of the ATG codon of ORF6 (Fig. 10A).

To define the 3′ end of ORF6 RNA expressed *in vitro*, 3′ RACE

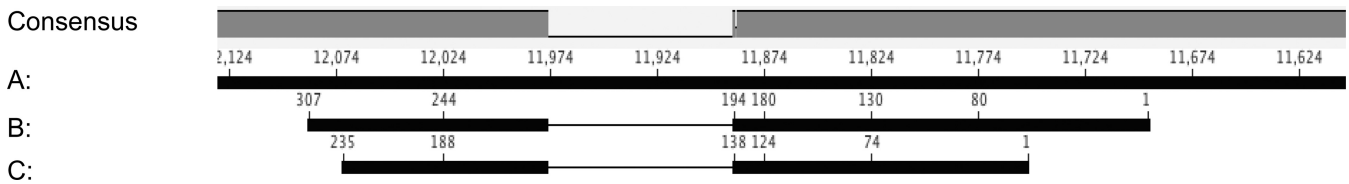

FIG 7 Alignment of intron splicing sites of CyHV-3 lytic and latent ORF6 transcripts with the CyHV-3 genome. The CyHV-3 genome with the predicted 86-bp intron (positions 11888 to 11974) (NCBI accession no. NC_009127.1) is shown. (A) CyHV-3 genomic DNA (NCBI accession no. NC_009127.1). (B) Sequence of RT-PCR product (310 bp) from lytic *in vitro* infection of CCB cells using primers ORF6s-F291 and ORF6s-R291. (C) Sequence of RT-PCR product (235 bp) from latently infected IgM$^+$ B cells using additional nested primers ORF6s-F216 and ORF6s-R216.

```
                                   * *        *                   *            *
                  *          *  * ** * *      *   **       ***    *  *         *   *
KHV ORF6      342 EEEEEASTSTTAATTTTPAPTSDAETEVPIKTEPQDTSCDEAATEDVKPDLAKLTAKPEEKPSKKPAKST 412
Cdd:PHA03378  683      TMLPIQWAPGTMQPPPRAPTPMRPP-AAPPGRAQRPAAATGRARPPAAAPGRA--RPPAAAPGRAR 745
Cdd:PHA03307  103 EGSPTPPGPSSPDPPPPTPPPASPPPSPAPDLSEMLRPVGSPGPPPAASP------PAAGASPAAVASDAA 167

                                *         *     *            *     *
                  ** *     *    **   * *  *     *      *   * ***** *   **  * *  ***  *
KHV ORF6      413 PPHQ----QPT---PPPHQPTPQPPQQPTKPQQSAQIPQHPAAPAPRQMPSQVPA-TSQAEGPPTPEQ 472
Cdd:PHA03378  746 PPAA----APGrarPPAAAPGRARPPAAA-PGAPTPQPPPQAPPAPQQRPRGAPTpQPPPQAGPTSMQ 808
Cdd:PHA03307  168 SSRQaalpLSS---PEETARAPSSPPAEPPPSTPP--AAASPRPPRRSSPISASA-SSPAPAPG     225
```

FIG 8 Alignment of ORF6 conserved domain with consensus sequences from the Conserved Domain Database (Cdd) (www.ncbi.nlm.nih.gov/Structure/cdd/cdd.shtml). PHA03378 is the Epstein-Barr nuclear antigen 3B consensus sequence derived from three gammaherpesvirus proteins. PHA03307 is the transcriptional regulator ICP4 consensus sequence derived from 36 alphaherpesvirus proteins. Residues in bold type are conserved; one asterisk above the ORF6 residue indicates consensus with one referenced domain, and two asterisks indicate consensus with both referenced domains. Lowercase letters indicate unaligned residues; dashes indicate variation in sequence length. The numbers before and after the amino acid sequence indicate the amount of sequence data that was imported from the complete consensus record (38).

was used. Similar to 5′ RACE, total RNA isolated from CyHV-3-infected CCB cells at 13 days p.i. was used. An oligo(dT) adapter primer was used to synthesize the cDNA. The resulting cDNA was amplified by PCR with AUAP and gene-specific primer 3RACE112. A product close to the predicted size was produced, but a nonspecific product was also amplified (Fig. 9, lane 1). The primary PCR product was reamplified with AUAP and a nested gene-specific primer 3RACE94, which amplified a 273-bp product from the 3′ end of the transcript (Fig. 9B, lane 2). Sequencing of this 273-bp product revealed a 189-nucleotide (nt) untranslated region (43) downstream of the stop codon; a polyadenylation signal was identified (AATAAA) 20 bp upstream of the 3′ end of the transcript (Fig. 10B).

DISCUSSION

In this study, CyHV-3 latency was investigated in IgM^{+} B cells that were sorted by monoclonal antibodies specific to common carp IgM using a magnetic column (Fig. 2 to 4). By real-time PCR, the presence of CyHV-3 in IgM^{+} B cells was found to be about 20-fold higher than in IgM^{-} WBC (Fig. 4). This suggests that at least one site of CyHV-3 latency is the IgM^{+} B cell. There are a variety of B cell subsets in teleost fish. In catfish (*Ictalurid* sp.), three B cell subsets have been identified: IgM^{+} IgD^{-}, IgM^{+} IgD^{+}, and IgM^{-} IgD^{+} B cells (44), while in rainbow trout, only two subsets have been described thus far: IgM^{+} IgD^{+} IgT^{-} and IgM^{-} IgD^{-} IgT^{+} B cells (45). In general, the circulating B cells have been shown to be more abundant in teleost fish than in humans. In most of the analyzed teleost fish species, B cells represent an average of ~30 to 60% of all peripheral blood leukocytes (PBL) (46). In contrast, the percentage of circulating B cells for humans is only ~2 to 8% of PBL (47). In koi, lymphocytes are categorized as small (<8 μm), medium (8 to 10 μm), or large (>10 μm) cells based on their diameter (48). The distribution of B cells within the peripheral WBC of common carp has not yet been well characterized. In our study, about 25% IgM^{+} B cells were recovered from the total peripheral WBC, which suggests that the IgM^{+} B cells may represent only a subset of circulating B cells of koi and common carp. The majority of CyHV-3 genome present during latent infection was detected in the IgM^{+} B cells, and very little was detected in the IgM^{-} WBC population, which is comprised of other B cell subsets, T cells, and other leukocytes (Fig. 4).

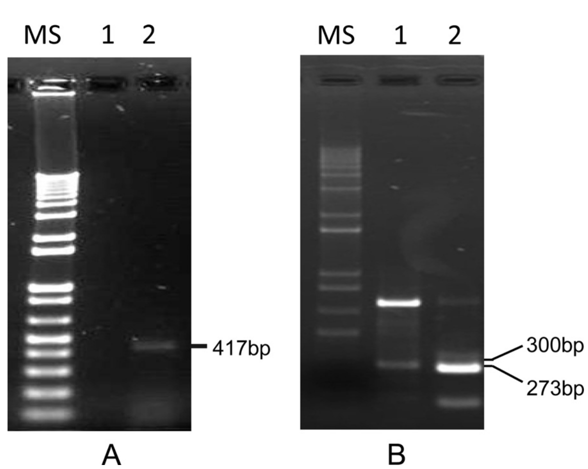

FIG 9 ORF6 RACE products generated by using RNA from CyHV-3-infected CCB cells at 13 days p.i. (A) 5′ RACE product amplified with primers ORF6-5RACE455 and AAP (lane 1) and seminested primers ORF6-5RACE293 and AUAP (lane 2). (B) 3′ RACE product amplified with primers ORF6-3RACE112 and AUAP (lane 1) and seminested primers ORF6-3RACE94 and AUAP (lane 2). The MS lanes contain molecular size markers (1Kb Plus; Invitrogen).

To confirm the identity of the IgM^{+} WBC selected by the magnetically activated cell sorting (MACS) microbeads as B cells, an antibody specific for a B cell transcription factor was used in our study. Transcription factor Pax5 is a master regulator of B cell development and has been identified in both mammalian and nonmammalian species (49, 50). Pax5 is mostly expressed in the vertebrate B cell lineage (51) including teleost fish species such as rainbow trout, puffer fish, and zebrafish (36, 52, 53). Within the B cell lineage, *Pax5* transcripts and their encoded products have been detected in pro-B, pre-B, and mature B cell lines, whereas either very low or undetectable levels were found in the various plasma cell lines studied (51). The functional domains of the Pax5 are highly conserved between vertebrate species (54). As shown in Fig. 2 and 3, the polyclonal anti-paired domain antibody ED-1 specific to trout Pax5 can cross-react with Pax5 of koi B cells. Visible Pax5 staining was also observed in some IgM^{-} cells (Fig. 3B and C), which suggests that IgM^{-} subsets of B cells may exist in koi. The expression of Pax5 was localized to the nucleus, as expected for a transcription regulator protein. Our study demon-

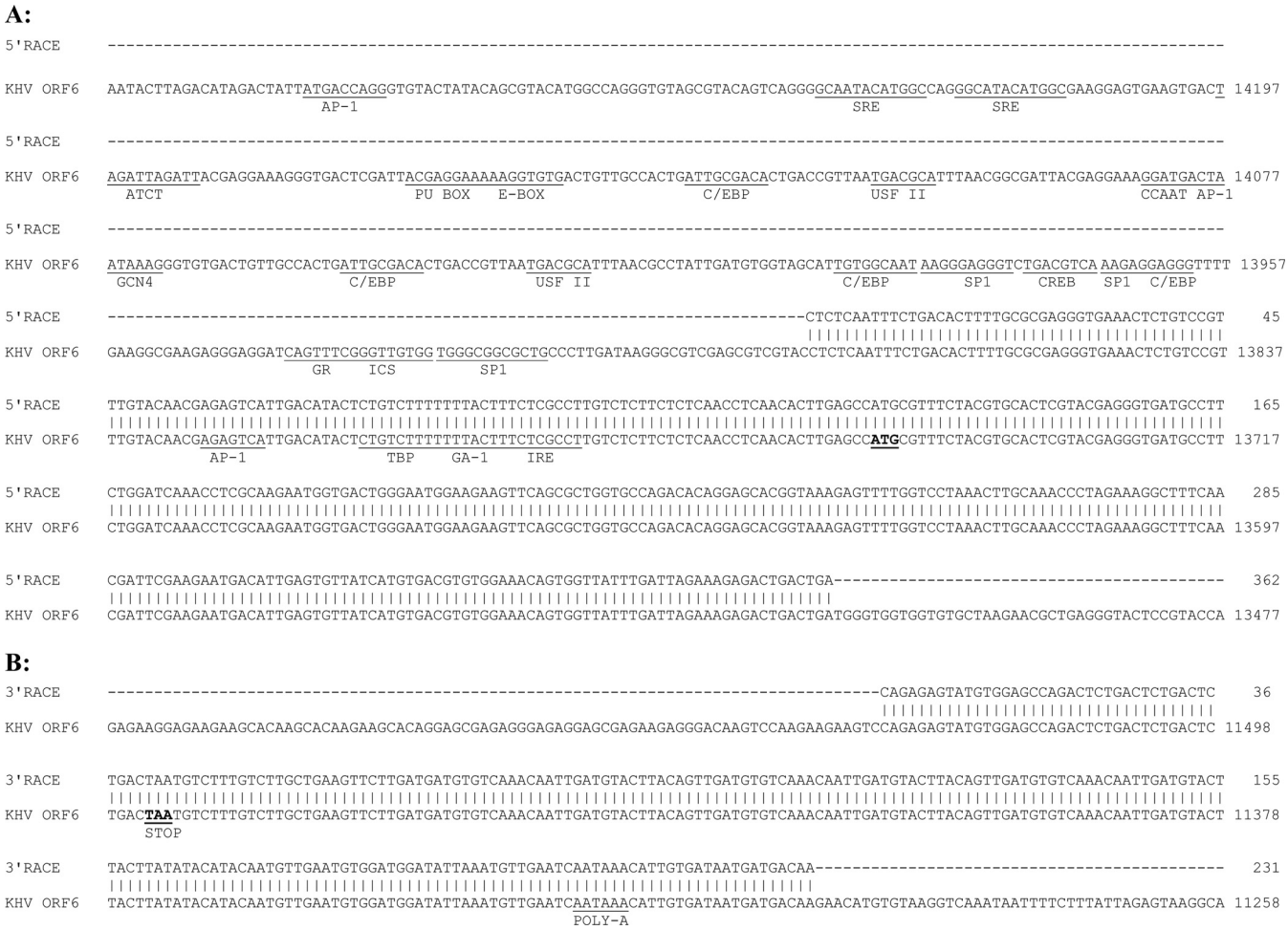

FIG 10 Sequence alignment of the ORF6 transcript ends with the CyHV-3 genome at ORF6 (NCBI accession no. NC_009127.1). The numbers before and after the sequence indicate the length of the genome that was imported from the complete consensus record. (A) 5′ RACE product mapped to the CyHV-3 genome. The numbers before and after the sequence indicate the length of the PCR product. The ATG start codon is shown underlined and in bold type. The underlined bases are predicted binding sites in the putative promoter region and can be cross-referenced in Table 2. (B) 3′ RACE product mapped to the CyHV-3 genome. The numbers before and after the sequence indicate the length of the PCR product. The TAA stop codon is shown underlined and in bold type. The predicted polyadenylation signal (AATAAA) is underlined. Alignments were performed using Geneious software.

strated that Pax5 is also expressed in common carp and can be used to identify B cells of common carp.

In this study, the transcript from ORF6 is shown to be expressed in B cells from latently infected koi. In latently infected fish, only the spliced CyHV-3 ORF6 transcript is detectable (Fig. 6). However, as shown in Fig. 7, both unspliced and spliced ORF6 transcripts are detectable during productive infection, wherein the unspliced transcripts are more abundant than the spliced ORF6 transcript as the productive infection progresses (Fig. 6A, 13 and 21 days p.i.). This is the first study to show that a spliced ORF6 transcript is abundantly expressed during CyHV-3 latency. It is possible that both spliced and unspliced ORF6 transcripts code for a protein and play a role in both productive and latent infections, whereas the spliced transcript alone is sufficient for latent infection. Future studies will have to address the roles of the translated products of spliced and unspliced ORF6 during the infection cycle.

A conserved domain (aa 342 to 472) identified in the predicted 725 aa of CyHV-3 ORF6 has homology to consensus sequences of EBNA-3B conserved domain (residues 683 to 808) and the N-terminal regulator domain of ICP4 (residues 103 to 225) (Fig. 8). EBNA is a family of Epstein-Barr virus (EBV) latent antigens which are only expressed in EBV latently infected B cells. It is interesting to discover that CyHV-3 expresses a gene during latency with a conserved domain with homology to EBNA-3B. During latency, EBV expresses three related nuclear proteins: EBNA-3A, -3B, and -3C, which are hypothesized to function as transcriptional transactivators. Both EBNA-3A and -3C genes are essential for EBV immortalization, but EBNA-3B is dispensable *in vitro* (55, 56). Since EBNA-3B is not necessary for EBV-induced B-cell immortalization *in vitro*, it is speculated that EBNA-3B is important for successful EBV infection *in vivo*, perhaps by regulating expression of cellular genes important for acute or latent EBV infection (41). It is possible that ORF6 plays a role similar to the role of EBNA-3B during latency of CyHV-3. Additionally, the conserved domain showed homology to the N-terminal regulator domain of ICP4, which is also a transcriptional transactivator and has homologs that can be found in many alphaherpesviruses (57–61). ICP4 contains discrete functional domains that determine DNA binding, dimerization, nuclear localization, and transcrip-

TABLE 2 Predicted binding sites in the putative promoter of ORF6 as labeled in Fig. 10

Label	Sequence (5′ to 3′)	Location from ATG[a]	Name	Length (no. of nucleotides)
AP1	GATGACTAAT	−330 to −321	Activator protein 1	10
	AGAGTCA	−72 to −66	Activator protein 1	7
	ATGACCAGG	−541 to −533	Activator protein 1	9
ATCT	TAGATTAGAT	−443 to −434	ATCT motif	10
C/EBP	TGTGGCAAT	−244 to −236	CCAAT box enhancer binding protein	9
	GAGGAGGG	−214 to −207	CCAAT box enhancer binding protein	8
	ATTGCGACA	−380 to −372	CCAAT box enhancer binding protein	9
	ATTGCGACA	−297 to −289	CCAAT box enhancer binding protein	9
CCAAT	GGATGACTAATAAAG	−331 to −317	CCAAT box	15
CREB	TGACGTCA	−224 to −217	Cyclic AMP response element	8
E BOX	AAAAGGTGTG	−403 to −394	E-box	10
GA-1	TTACTTTCT	−45 to −37	GA-1	9
GCN4	ATGACTAAT	−329 to −321	GCN4 recognition site	9
GR	CAGTTTCGGGTTGTGG	−183 to −168	Glucocorticoid receptor	16
ICS	AGTTTCGGGTTG	−182 to −171	Interferon consensus sequence	12
IRE	TACTTTCTCGCCT	−44 to −32	Insulin response element	13
PU BOX	ACGAGGAAAA	−410 to −401	PU box	10
SP1	TGGGCGGCGCTG	−167 to −156	Specificity protein 1	12
	AAGGGAGGGT	−235 to −226	Specificity protein 1	10
	AAGAGGAGGG	−216 to −207	Specificity protein 1	10
SRE	GCAATACATGGC	−486 to −475	Serum response element	12
	GGCATACATGGC	−471 to −460	Serum response element	12
TBP	CTGTCTTTTTTTACTTT	−55 to −39	Tata box binding protein	17
USF II	TGACGCA	−360 to −354	Upstream stimulatory factor	7
	TGACGCA	−277 to −271	Upstream stimulatory factor	7

[a] The mapped location is the number of nucleotides upstream from the ATG start site.

tional activation (62). It is interesting to find that ORF6 contains a conserved domain with homology to the ICP4 transcription activation regulatory domain near the amino terminus (residues 143 to 210) which are necessary for ICP4 function (62). This suggests that the conserved domain in ORF6 may be essential for transcription activation, and ORF6 may function as a transcription activator, perhaps by regulating expression of cellular genes important for acute or latent CyHV-3 infection.

Based on the transcription regulatory site search by Softberry, many transcription regulatory elements are found to be present in the putative ORF6 promoter as illustrated in Fig. 10A and Table 2. An E-box binding site is present −403 to −394 nt upstream of the ATG codon, which normally regulates responses to cell growth and differentiation, apoptosis, and immune response (63–65). There are three activator protein 1 (AP-1) binding sites upstream of the ATG codon of ORF6, which regulate gene expression in response to a variety of stimuli, including cytokines, growth factors, stressors, and bacterial and viral infections (66, 67). Two serum response elements (SRE), which are binding sites of serum response factor (SRF), were also present in the promoter region. SRF normally regulates the activity of many immediate early genes, for example c-*fos*, and thereby participates in cell cycle regulation, apoptosis, cell growth, and cell differentiation (68). This suggests that ORF6 expression can be regulated under many conditions, such as cell growth, cell differentiation, apoptosis, immune responses, and bacterial and viral infections. A number of promoter regulatory elements found in the HSV-1 LAT promoter were also present in the putative ORF6 promoter (69). These elements include a cyclic AMP response element binding site (CREB), a CCAAT box, three Sp1 DNA-binding consensus sequences, and two upstream stimulatory factor (USF) binding sites (69). In addition, a glucocorticoid receptor (GR) binding site is also present in the ORF6 promoter region; it has been shown that GR is associated with cortisol-induced reactivation of BHV-1 from latency (70). Similar to the EBV LMP1 promoter regulatory region, a PU box and GCN4 binding site are present in ORF6 putative promoter region (50). This suggests the ORF6 promoter may be regulated in a manner similar to that of LAT, LR, and LMP1 during latency. Up to four CCAAT-enhancer-binding protein (C/EBP) or NF-IL-6 (nuclear factor for interleukin 6 [IL-6] expression) binding sites are predicted in the ORF6 promoter region. NF-IL-6 has roles in regulation of IL-6 and genes involved in acute-phase reaction, inflammation, and hematopoiesis (71, 72). It will be interesting to discover what role NF-IL-6 plays in CyHV-3 ORF6 gene expression during latency. Additional transcription binding sites for insulin response (IRE), interferon response (73), and oxidative stress (GA-1) were also present in the ORF6 putative promoter region. These binding sites suggest that

the ORF6 gene can be regulated by many host transcription factors involved in cell growth and immune response and viral transcription factors during infection. It will be interesting to find how each of the regulatory elements functions during acute and latent CyHV-3 infection.

In summary, this is the first report of identification of CyHV-3 latency in B cells and gene transcription during latency for a herpesvirus in the *Alloherpesviridae*. The hypothetical protein sequence of ORF6 contains a conserved domain, which has homology to a conserved domain of EBNA-3B and ICP4. These data suggest that ORF6 may have a conserved function similar to those of EBNA-3B and ICP4 and may play a critical role in the mechanism and evolution of herpesvirus latency.

ACKNOWLEDGMENTS

We thank the American Koi Club Association for funding this study. A. N. Reed was supported by Office of the Director of the National Institutes of Health T32 training grant RR023917 and grant T32OD011020.

The contents of this article are solely the responsibility of the authors and do not necessarily represent the official views of the National Institutes of Health.

We thank Ronald Hedrick (University of California, Davis) for providing the KF-1 cell line and KHV-U strains used in this study. We thank Barbara Taylor for assistance with confocal microscopy. We thank Patty Zwollo (College of William and Mary) for providing the Pax5 antibody used in this study. We also thank George Rohrmann and Sara Weed for helping to edit the paper. We wish to acknowledge the Confocal Microscopy Facility of the Center for Genome Research and Biocomputing and the Environmental and Health Sciences Center at Oregon State University.

REFERENCES

1. **Gilad O, Yun S, Andree KB, Adkison MA, Zlotkin A, Bercovier H, Eldar A, Hedrick RP.** 2002. Initial characteristics of koi herpesvirus and development of a polymerase chain reaction assay to detect the virus in koi, Cyprinus carpio koi. Dis. Aquat. Organ. **48:**101–108. http://dx.doi.org/10.3354/dao048101.
2. **Gilad O, Yun S, Zagmutt-Vergara FJ, Leutenegger CM, Bercovier H, Hedrick RP.** 2004. Concentrations of a koi herpesvirus (KHV) in tissues of experimentally infected Cyprinus carpio koi as assessed by real-time TaqMan PCR. Dis. Aquat. Organ. **60:**179–187. http://dx.doi.org/10.3354/dao060179.
3. **Bondad-Reantaso MG, Sunarto A, Subasinghe RP.** 2007. Managing the koi herpesvirus disease outbreak in Indonesia and the lessons learned. Dev. Biol. (Basel) **129:**21–28.
4. **Grimmett SG, Warg JV, Getchell RG, Johnson DJ, Bowser PR.** 2006. An unusual koi herpesvirus associated with a mortality event of common carp Cyprinus carpio in New York State, USA. J. Wildl. Dis. **42:**658–662. http://dx.doi.org/10.7589/0090-3558-42.3.658.
5. **Iida T, Sano M.** 2005. Koi herpesvirus disease. Uirusu **55:**145–151. (In Japanese.) http://dx.doi.org/10.2222/jsv.55.145.
6. **Waltzek TB, Kelley GO, Stone DM, Way K, Hanson L, Fukuda H, Hirono I, Aoki T, Davison AJ, Hedrick RP.** 2005. Koi herpesvirus represents a third cyprinid herpesvirus (CyHV-3) in the family Herpesviridae. J. Gen. Virol. **86:**1659–1667. http://dx.doi.org/10.1099/vir.0.80982-0.
7. **Davison AJ, Kurobe T, Gatherer D, Cunningham C, Korf I, Fukuda H, Hedrick RP, Waltzek TB.** 2013. Comparative genomics of carp herpesviruses. J. Virol. **87:**2908–2922. http://dx.doi.org/10.1128/JVI.03206-12.
8. **St-Hilaire S, Beevers N, Joiner C, Hedrick RP, Way K.** 2009. Antibody response of two populations of common carp, Cyprinus carpio L., exposed to koi herpesvirus. J. Fish Dis. **32:**311–320. http://dx.doi.org/10.1111/j.1365-2761.2008.00993.x.
9. **Eide KE, Miller-Morgan T, Heidel JR, Kent ML, Bildfell RJ, Lapatra S, Watson G, Jin L.** 2011. Investigation of koi herpesvirus latency in koi. J. Virol. **85:**4954–4962. http://dx.doi.org/10.1128/JVI.01384-10.
10. **Cohrs R, Gilden D.** 2011. Alphaherpesvirus latency. J. Neurovirol. **17:**509–511. http://dx.doi.org/10.1007/s13365-011-0075-9.
11. **Jones C, Delhon G, Bratanich A, Kutish G, Rock D.** 1990. Analysis of the transcriptional promoter which regulates the latency-related transcript of bovine herpesvirus 1. J. Virol. **64:**1164–1170.
12. **Priola SA, Stevens JG.** 1991. The 5′ and 3′ limits of transcription in the pseudorabies virus latency associated transcription unit. Virology **182:**852–856. http://dx.doi.org/10.1016/0042-6822(91)90628-O.
13. **Jones C.** 2003. Herpes simplex virus type 1 and bovine herpesvirus 1 latency. Clin. Microbiol. Rev. **16:**79–95. http://dx.doi.org/10.1128/CMR.16.1.79-95.2003.
14. **Grinde B.** 2013. Herpesviruses: latency and reactivation - viral strategies and host response. J. Oral Microbiol. **5:**22766. http://dx.doi.org/10.3402/jom.v5i0.22766.
15. **Jin L, Scherba G.** 1999. Expression of the pseudorabies virus latency-associated transcript gene during productive infection of cultured cells. J. Virol. **73:**9781–9788.
16. **Stevens JG, Haarr L, Porter DD, Cook ML, Wagner EK.** 1988. Prominence of the herpes simplex virus latency-associated transcript in trigeminal ganglia from seropositive humans. J. Infect. Dis. **158:**117–123. http://dx.doi.org/10.1093/infdis/158.1.117.
17. **Jin L, Schnitzlein WM, Scherba G.** 2000. Identification of the pseudorabies virus promoter required for latency-associated transcript gene expression in the natural host. J. Virol. **74:**6333–6338. http://dx.doi.org/10.1128/JVI.74.14.6333-6338.2000.
18. **Zwaagstra JC, Ghiasi H, Nesburn AB, Wechsler SL.** 1991. Identification of a major regulatory sequence in the latency associated transcript (LAT) promoter of herpes simplex virus type 1 (HSV-1). Virology **182:**287–297. http://dx.doi.org/10.1016/0042-6822(91)90672-X.
19. **Krause PR, Ostrove JM, Straus SE.** 1991. The nucleotide sequence, 5′ end, promoter domain, and kinetics of expression of the gene encoding the herpes simplex virus type 2 latency-associated transcript. J. Virol. **65:**5619–5623.
20. **Sadzot-Delvaux C, Kinchington PR, Debrus S, Rentier B, Arvin AM.** 1997. Recognition of the latency-associated immediate early protein IE63 of varicella-zoster virus by human memory T lymphocytes. J. Immunol. **159:**2802–2806.
21. **Cheung AK, Abendroth A, Cunningham AL, Slobedman B.** 2006. Viral gene expression during the establishment of human cytomegalovirus latent infection in myeloid progenitor cells. Blood **108:**3691–3699. http://dx.doi.org/10.1182/blood-2005-12-026682.
22. **Goodrum FD, Jordan CT, High K, Shenk T.** 2002. Human cytomegalovirus gene expression during infection of primary hematopoietic progenitor cells: a model for latency. Proc. Natl. Acad. Sci. U. S. A. **99:**16255–16260. http://dx.doi.org/10.1073/pnas.252630899.
23. **Kondo K, Xu J, Mocarski ES.** 1996. Human cytomegalovirus latent gene expression in granulocyte-macrophage progenitors in culture and in seropositive individuals. Proc. Natl. Acad. Sci. U. S. A. **93:**11137–11142. http://dx.doi.org/10.1073/pnas.93.20.11137.
24. **Kondo K, Mocarski ES.** 1995. Cytomegalovirus latency and latency-specific transcription in hematopoietic progenitors. Scand. J. Infect. Dis. Suppl. **99:**63–67.
25. **Goodrum F, Reeves M, Sinclair J, High K, Shenk T.** 2007. Human cytomegalovirus sequences expressed in latently infected individuals promote a latent infection in vitro. Blood **110:**937–945. http://dx.doi.org/10.1182/blood-2007-01-070078.
26. **Niedobitek G, Agathanggelou A, Steven N, Young LS.** 2000. Epstein-Barr virus (EBV) in infectious mononucleosis: detection of the virus in tonsillar B lymphocytes but not in desquamated oropharyngeal epithelial cells. Mol. Pathol. **53:**37–42. http://dx.doi.org/10.1136/mp.53.1.37.
27. **Speck SH, Ganem D.** 2010. Viral latency and its regulation: lessons from the gamma-herpesviruses. Cell Host Microbe **8:**100–115. http://dx.doi.org/10.1016/j.chom.2010.06.014.
28. **Olsen SJ, Sarid R, Chang Y, Moore PS.** 2000. Evaluation of the latency-associated nuclear antigen (ORF73) of Kaposi's sarcoma-associated herpesvirus by peptide mapping and bacterially expressed recombinant Western blot assay. J. Infect. Dis. **182:**306–310. http://dx.doi.org/10.1086/315689.
29. **Knickelbein JE, Khanna KM, Yee MB, Baty CJ, Kinchington PR, Hendricks RL.** 2008. Noncytotoxic lytic granule-mediated CD8+ T cell inhibition of HSV-1 reactivation from neuronal latency. Science **322:**268–271. http://dx.doi.org/10.1126/science.1164164.
30. **Perng GC, Jones C, Ciacci-Zanella J, Stone M, Henderson G, Yukht A, Slanina SM, Hofman FM, Ghiasi H, Nesburn AB, Wechsler SL.** 2000. Virus-induced neuronal apoptosis blocked by the herpes simplex virus

latency-associated transcript. Science **287:**1500–1503. http://dx.doi.org/10.1126/science.287.5457.1500.
31. **Jenkins C, Garcia W, Godwin MJ, Spencer JV, Stern JL, Abendroth A, Slobedman B.** 2008. Immunomodulatory properties of a viral homolog of human interleukin-10 expressed by human cytomegalovirus during the latent phase of infection. J. Virol. **82:**3736–3750. http://dx.doi.org/10.1128/JVI.02173-07.
32. **Reeves MB, Sinclair JH.** 2010. Analysis of latent viral gene expression in natural and experimental latency models of human cytomegalovirus and its correlation with histone modifications at a latent promoter. J. Gen. Virol. **91:**599–604. http://dx.doi.org/10.1099/vir.0.015602-0.
33. **St-Hilaire S, Beevers N, Way K, Le Deuff RM, Martin P, Joiner C.** 2005. Reactivation of koi herpesvirus infections in common carp Cyprinus carpio. Dis. Aquat. Organ. **67:**15–23. http://dx.doi.org/10.3354/dao067015.
34. **Xu JR, Bently J, Beck L, Reed A, Miller-Morgan T, Heidel JR, Kent ML, Rockey DD, Jin L.** 2013. Analysis of koi herpesvirus latency in wild common carp and ornamental koi in Oregon, USA. J. Virol. Methods **187:**372–379. http://dx.doi.org/10.1016/j.jviromet.2012.11.015.
35. **Zwollo P, Rao S, Wallin JJ, Gackstetter ER, Koshland ME.** 1998. The transcription factor NF-kappaB/p50 interacts with the blk gene during B cell activation. J. Biol. Chem. **273:**18647–18655. http://dx.doi.org/10.1074/jbc.273.29.18647.
36. **Zwollo P, Haines A, Rosato P, Gumulak-Smith J.** 2008. Molecular and cellular analysis of B-cell populations in the rainbow trout using Pax5 and immunoglobulin markers. Dev. Comp. Immunol. **32:**1482–1496. http://dx.doi.org/10.1016/j.dci.2008.06.008.
37. **Aoki T, Hirono I, Kurokawa K, Fukuda H, Nahary R, Eldar A, Davison AJ, Waltzek TB, Bercovier H, Hedrick RP.** 2007. Genome sequences of three koi herpesvirus isolates representing the expanding distribution of an emerging disease threatening koi and common carp worldwide. J. Virol. **81:**5058–5065. http://dx.doi.org/10.1128/JVI.00146-07.
38. **Marchler-Bauer A, Lu S, Anderson JB, Chitsaz F, Derbyshire MK, DeWeese-Scott C, Fong JH, Geer LY, Geer RC, Gonzales NR, Gwadz M, Hurwitz DI, Jackson JD, Ke Z, Lanczycki CJ, Lu F, Marchler GH, Mullokandov M, Omelchenko MV, Robertson CL, Song JS, Thanki N, Yamashita RA, Zhang D, Zhang N, Zheng C, Bryant SH.** 2011. CDD: a Conserved Domain Database for the functional annotation of proteins. Nucleic Acids Res. **39:**D225–D229. http://dx.doi.org/10.1093/nar/gkq1189.
39. **Ambinder RF, Mullen MA, Chang YN, Hayward GS, Hayward SD.** 1991. Functional domains of Epstein-Barr virus nuclear antigen EBNA-1. J. Virol. **65:**1466–1478.
40. **Sjoblom A, Nerstedt A, Jansson A, Rymo L.** 1995. Domains of the Epstein-Barr virus nuclear antigen 2 (EBNA2) involved in the transactivation of the latent membrane protein 1 and the EBNA Cp promoters. J. Gen. Virol. **76**(Part 11)**:**2669–2678. http://dx.doi.org/10.1099/0022-1317-76-11-2669.
41. **Jiang H, Cho YG, Wang F.** 2000. Structural, functional, and genetic comparisons of Epstein-Barr virus nuclear antigen 3A, 3B, and 3C homologues encoded by the rhesus lymphocryptovirus. J. Virol. **74:**5921–5932. http://dx.doi.org/10.1128/JVI.74.13.5921-5932.2000.
42. **Lee LY, Schaffer PA.** 1998. A virus with a mutation in the ICP4-binding site in the L/ST promoter of herpes simplex virus type 1, but not a virus with a mutation in open reading frame P, exhibits cell-type-specific expression of gamma(1)34.5 transcripts and latency-associated transcripts. J. Virol. **72:**4250–4264.
43. **Brutlag DL, Dautricourt J-P, Maulik S, Relph J.** 1990. Sensitive similarity searches of biological sequence databases. Comput. Appl. Biosci. **6:**237–245.
44. **Edholm ES, Bengten E, Stafford JL, Sahoo M, Taylor EB, Miller NW, Wilson M.** 2010. Identification of two IgD+ B cell populations in channel catfish, Ictalurus punctatus. J. Immunol. **185:**4082–4094. http://dx.doi.org/10.4049/jimmunol.1000631.
45. **Zhang YA, Salinas I, Li J, Parra D, Bjork S, Xu Z, LaPatra SE, Bartholomew J, Sunyer JO.** 2010. IgT, a primitive immunoglobulin class specialized in mucosal immunity. Nat. Immunol. **11:**827–835. http://dx.doi.org/10.1038/ni.1913.
46. **Sunyer JO.** 2012. Evolutionary and functional relationships of B cells from fish and mammals: insights into their novel roles in phagocytosis and presentation of particulate antigen. Infect. Disord. Drug Targets **12:**200–212. http://dx.doi.org/10.2174/187152612800564419.
47. **de Jong JL, Zon LI.** 2005. Use of the zebrafish system to study primitive and definitive hematopoiesis. Annu. Rev. Genet. **39:**481–501. http://dx.doi.org/10.1146/annurev.genet.39.073003.095931.
48. **Tripathi NK, Latimer KS, Burnley VV.** 2004. Hematologic reference intervals for koi (Cyprinus carpio), including blood cell morphology, cytochemistry, and ultrastructure. Vet. Clin. Pathol. **33:**74–83. http://dx.doi.org/10.1111/j.1939-165X.2004.tb00353.x.
49. **Adams B, Dorfler P, Aguzzi A, Kozmik Z, Urbanek P, Maurer-Fogy I, Busslinger M.** 1992. Pax-5 encodes the transcription factor BSAP and is expressed in B lymphocytes, the developing CNS, and adult testis. Genes Dev. **6:**1589–1607. http://dx.doi.org/10.1101/gad.6.9.1589.
50. **Zwollo P.** 2011. Dissecting teleost B cell differentiation using transcription factors. Dev. Comp. Immunol. **35:**898–905. http://dx.doi.org/10.1016/j.dci.2011.01.009.
51. **Cobaleda C, Schebesta A, Delogu A, Busslinger M.** 2007. Pax5: the guardian of B cell identity and function. Nat. Immunol. **8:**463–470. http://dx.doi.org/10.1038/ni1454.
52. **Ohtani M, Miyadai T, Hiroishi S.** 2006. Identification of genes encoding critical factors regulating B-cell terminal differentiation in torafugu (Takifugu rubripes). Comp. Biochem. Physiol. Part D Genomics Proteomics **1:**109–114. http://dx.doi.org/10.1016/j.cbd.2005.10.003.
53. **Pfeffer PL, Gerster T, Lun K, Brand M, Busslinger M.** 1998. Characterization of three novel members of the zebrafish Pax2/5/8 family: dependency of Pax5 and Pax8 expression on the Pax2.1 (noi) function. Development **125:**3063–3074.
54. **Barr M, Mott K, Zwollo P.** 2011. Defining terminally differentiating B cell populations in rainbow trout immune tissues using the transcription factor XbpI. Fish Shellfish Immunol. **31:**727–735. http://dx.doi.org/10.1016/j.fsi.2011.06.018.
55. **Tomkinson B, Kieff E.** 1992. Second-site homologous recombination in Epstein-Barr virus: insertion of type 1 EBNA 3 genes in place of type 2 has no effect on in vitro infection. J. Virol. **66:**780–789.
56. **Tomkinson B, Kieff E.** 1992. Use of second-site homologous recombination to demonstrate that Epstein-Barr virus nuclear protein 3B is not important for lymphocyte infection or growth transformation in vitro. J. Virol. **66:**2893–2903.
57. **Fuchs W, Ehrlich C, Klupp BG, Mettenleiter TC.** 2000. Characterization of the replication origin (Ori(S)) and adjoining parts of the inverted repeat sequences of the pseudorabies virus genome. J. Gen. Virol. **81:**1539–1543.
58. **Kenyon TK, Lynch J, Hay J, Ruyechan W, Grose C.** 2001. Varicella-zoster virus ORF47 protein serine kinase: characterization of a cloned, biologically active phosphotransferase and two viral substrates, ORF62 and ORF63. J. Virol. **75:**8854–8858. http://dx.doi.org/10.1128/JVI.75.18.8854-8858.2001.
59. **Grundy FJ, Baumann RP, O'Callaghan DJ.** 1989. DNA sequence and comparative analyses of the equine herpesvirus type 1 immediate early gene. Virology **172:**223–236. http://dx.doi.org/10.1016/0042-6822(89)90124-4.
60. **Afonso CL, Tulman ER, Lu Z, Zsak L, Rock DL, Kutish GF.** 2001. The genome of turkey herpesvirus. J. Virol. **75:**971–978. http://dx.doi.org/10.1128/JVI.75.2.971-978.2001.
61. **Van Opdenbosch N, Van den Broeke C, De Regge N, Tabares E, Favoreel HW.** 2012. The IE180 protein of pseudorabies virus suppresses phosphorylation of translation initiation factor eIF2alpha. J. Virol. **86:**7235–7240. http://dx.doi.org/10.1128/JVI.06929-11.
62. **Bates PA, DeLuca NA.** 1998. The polyserine tract of herpes simplex virus ICP4 is required for normal viral gene expression and growth in murine trigeminal ganglia. J. Virol. **72:**7115–7124.
63. **Carter RS, Ordentlich P, Kadesch T.** 1997. Selective utilization of basic helix-loop-helix-leucine zipper proteins at the immunoglobulin heavy-chain enhancer. Mol. Cell. Biol. **17:**18–23.
64. **Giangrande PH, Hallstrom TC, Tunyaplin C, Calame K, Nevins JR.** 2003. Identification of E-box factor TFE3 as a functional partner for the E2F3 transcription factor. Mol. Cell. Biol. **23:**3707–3720. http://dx.doi.org/10.1128/MCB.23.11.3707-3720.2003.
65. **Giangrande PH, Zhu W, Rempel RE, Laakso N, Nevins JR.** 2004. Combinatorial gene control involving E2F and E box family members. EMBO J. **23:**1336–1347. http://dx.doi.org/10.1038/sj.emboj.7600134.
66. **Ameyar M, Wisniewska M, Weitzman JB.** 2003. A role for AP-1 in apoptosis: the case for and against. Biochimie **85:**747–752. http://dx.doi.org/10.1016/j.biochi.2003.09.006.
67. **Sanyal S, Sandstrom DJ, Hoeffer CA, Ramaswami M.** 2002. AP-1 functions upstream of CREB to control synaptic plasticity in Drosophila. Nature **416:**870–874. http://dx.doi.org/10.1038/416870a.
68. **Norman C, Runswick M, Pollock R, Treisman R.** 1988. Isolation and properties of cDNA clones encoding SRF, a transcription factor that binds

to the c-fos serum response element. Cell **55:**989–1003. http://dx.doi.org/10.1016/0092-8674(88)90244-9.

69. **Kenny JJ, Millhouse S, Wotring M, Wigdahl B.** 1997. Upstream stimulatory factor family binds to the herpes simplex virus type 1 latency-associated transcript promoter. Virology **230:**381–391. http://dx.doi.org/10.1006/viro.1997.8501.
70. **Frizzo da Silva L, Kook I, Doster A, Jones C.** 2013. Bovine herpesvirus 1 regulatory proteins bICP0 and VP16 are readily detected in trigeminal ganglionic neurons expressing the glucocorticoid receptor during the early stages of reactivation from latency. J. Virol. **87:**11214–11222. http://dx.doi.org/10.1128/JVI.01737-13.
71. **Akira S, Isshiki H, Sugita T, Tanabe O, Kinoshita S, Nishio Y, Nakajima T, Hirano T, Kishimoto T.** 1990. A nuclear factor for IL-6 expression (NF-IL6) is a member of a C/EBP family. EMBO J. **9:**1897–1906.
72. **Hirano T, Akira S, Taga T, Kishimoto T.** 1990. Biological and clinical aspects of interleukin 6. Immunol. Today **11:**443–449. http://dx.doi.org/10.1016/0167-5699(90)90173-7.
73. **Smith GE, Ju G, Ericson BL, Moschera J, Lahm H, Chizzonite R, Summers MD.** 1985. Modification and secretion of human interleukin 2 produced in insect cells by a baculovirus expression vector. Proc. Natl. Acad. Sci. U. S. A. **82:**8404–8408. http://dx.doi.org/10.1073/pnas.82.24.8404.